11th Australasian Fluid Mechanics Conference
University of Tasmania, Hobart, Australia
14-18 December 1992

FLOW CHARACTERISTICS AROUND TWO CROSSED CIRCULAR CYLINDERS

Hidemi YAMADA and Hideo OSAKA

Department of Mechanical Engineering
Yamaguchi University
Tokiwadai, Ube 755, JAPAN

ABSTRACT

The flow around two circular cylinders forming a cross in contact with each other, set normal to the uniform stream, was investigated experimentally from the measurements of surface pressure distributions and the frequency of the vortex shedding from the two cylinders at a Reynolds number of 4×10^3. The local drag coefficient of each cylinder was estimated from the surface distribution on the circumference.

Since there was a the bleed flow near the contact point, the primary separation line, the contour map of the surface pressure and the local drag coefficient in the region of about $y/d\leqq4$ and $z/d\leqq4$ was considerably different from the other region, respectively. The vortex shedding frequency of the four cylinder parts away from the contact point was almost equal to that in a single cylinder, but the phase of these shedding vortices was not correlated with each other.

NOTATION

d: Circular cylinder diameter
θ: Circumference degree of circular cylinder
Uo: Free stream velocity
Po: Free stream static pressure
P: Surface pressure of circular cylinder
Cp: Surface pressure coefficient,
$Cp=(P-Po)/(\rho Uo^2/2)$
Cd: Local pressure drag coefficient,
$Cd=(1/2)\int_0^{2\pi}Cp\cos\theta\,d\theta$
Rd: Experimental Reynolds number, $Rd=Uod/\nu$
Cd_z: Pressure drag coefficient of single cylinder

INTRODUCTION

The flow interference in the cross region of two effectively long circular cylinders which overlap perpendicular to each other represents the most basic type of flow through members of lattice structures such as off-shore structures, screens and turbulent grids forming a interwoven wire, and new type of heat exchangers.

Zdravkovich(1983) measured the pressure distribution and the flow pattern on the surface of two circular cylinders forming a cross, and referred to the spanwise variation of the local pressure drag coefficients and the surface flow pattern in detail. But, the flow field around the cross region seems to be under the influence of both the small aspect ratio and the high blockage ratio. Recently, the turbulent intensity and the vorticity distributions in the near wake behind the two cylinders forming a cross for various cylinder spacings and the surface pressure distribution at the center of one were measured with large aspect and low blockage ratios (Fox & Toy, 1988a, b, Fox, 1991). They suggest the presence of streamwise vortices in the near wake and vortex formation in a gap of the two cylinders. But the spanwise variation of the surface flow was hardly mentioned.

The aims of this paper are to clarify in detail the surface flow pattern on two circular cylinders over a wide spanwise range, to find the relationship between surface flow and the spanwise variation of the local drag coefficient. Furthermore, the phase relation between the vortices shed from the four cylinder parts away from the contact point is examined.

EXPERIMENTAL APPARATUS

The wind tunnel used in this experiment has a working cross section of about 400mm square. The aspect ratio of two circular cylinders forming a criss-cross in the center of the working cross section is 76, since the two cylinders have a diameter of d=5mm, except in the flow visualization, and the four end disks were positioned 10mm away from the tunnel walls. The experimental Reynolds number was kept to 4×10^3 for the measurements of surface pressure and wake velocity. The pressure distribution on the cylinder surface was measured by a tapping hole with 0.3mm in diameter. The fluctuating velocity in the wake was measured by an I-type hot wire anemometer system, the energy spectrum and the correlation of fluctuating velocity were processed by the a digital correlator.

The flow pattern on the cylinder surface was observed by the oil-film method. In this method, a stainless steel with a thickness of $30\mu m$ was coated with black paint and was wound up into the two 32mm diameter cylinders which were set in the uniform flow of Uo=10m/s.

To observe the vortex shedding pattern from the two cylinders, an open channel type water tunnel with a working cross section of about 400mm square and 10mm diameter circular cylinders with many 0.3mm diameter holes for dye injection in the positions of θ=180° were employed.

RESULTS AND DISCUSSIONS

Pressure distribution on cylinder surface

Fig. 2(a), (b) show the distribution of the surface pressure Cp on the circumference in each spanwise position of the upstream cylinder and the downstream cylinder respectively. The surface pressure distributions on the rear side of the upstream cylinder and on the front side of the downstream cylinder in the vicinity of the cross region are very different from the rest. On the other hand, the surface pressure does not vary greatly in the frontal range of about $\theta \leqq 60°$ in the upstream cylinder. Since there is a high speed fluid flow towards the vicinity of the contact point by the necklace vortex, which is formed in the upstream region of the downstream cylinder, the surface pressure coefficient distribution on the symmetry plane of y/d=0 in the upstream cylinder has a peak value at about θ=170°.

Fig. 3(a), (b), (c) show the oil-film pattern on the surface of the stainless sheet which has been wound off and spread, the flow direction sketch and the contour map of the surface pressure on the upstream circular cylinder, respectively. It is known from Fig. 3(a) that the primary separation line has a tendency to go back, except the center region of the span, as y/d decreases. In the region A of about $-0.5 \leqq y/d \leqq 0.5$ as shown in Fig. 3(b), a necklace vortex with a small cross section is formed downstream of the arch-shaped separation line. The necklace vortex separates from the cylinder surface in about y/d=0.5 and θ =150°, and issues behind the upstream cylinder. The fluid flow in the region B beyond the necklace vortex separates from the cylinder surface on the line between about (y/d, θ)=(0, 180°) and (0.5, 150°), and issues as bleed flow towards the corner of the cross region. This bleed flow would perhaps generate the patterns of region C in Fig. 3(b) and region E in Fig. 4(b). Therefore, in region C the secondary flow towards the outside mainly along the y axis is formed. In region D a secondary flow in the direction of the contact point is observed. The contour map shows that the spanwise variation of the surface pressure distribution in the range of about $y/d \geqq 4$ and $z/d \geqq 4$ is very small. In addition, in the neighborhood of about y/d=1 and θ=130° there is a significant minimum pressure region which can be expected to correlate with the streamwise vortex formation region.

Fig. 4(a), (b), (c) show the oil-film pattern on the surface of the stainless sheet, the flow direction sketch and the contour map of the surface pressure on the downstream circular cylinder, respectively. Fig. 4(a) shows that the primary separation line has a tendency to go ahead as y/d decreases. In particular the primary separation line curves rapidly at about z/d=0.25. Therefore, the surface flow in the range of about $z/d \leqq 0.25$ is much different from that of the other spanwise region as shown by Zdravkovich. Particularly, the bleed flow region E in the spanwise range of $z/d \leqq 0.25$ exhibits a shape of rhombus. It may be found that on the z/d=0 plane in the region E the bleed flow begins to blow in the position of about θ=30° and separates at about θ=110°. The contour map of surface pressure is corresponded to the oil-film pattern mentioned above. In addition, the minimum pressure region of about z/d=1 on the rear side of the downstream cylinder may be expected to be significant as the foot region of the streamwise vortex.

Fig. 5 shows the spanwise variation of the primary separation line obtained as the position of the minimum pressure on the surface pressure distribution of the upstream and downstream cylin-

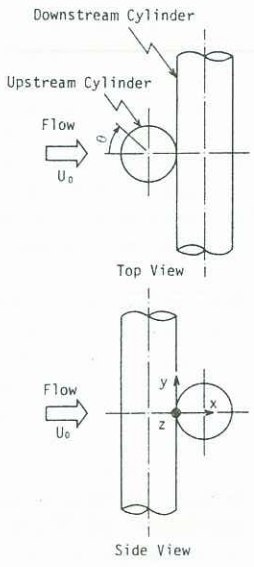

Fig. 1 Coordinate system

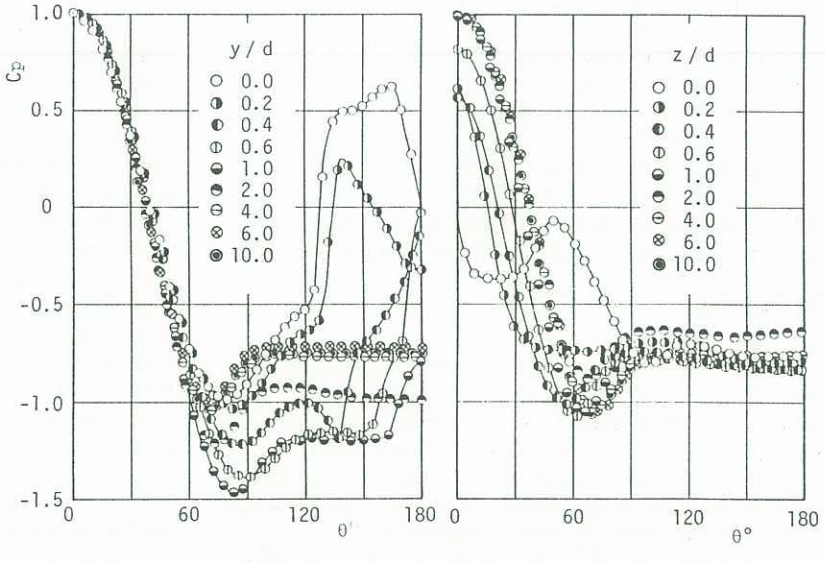

(a) Upstream cylinder (b) Downstream cylinder

Fig. 2 Surface pressure distributions

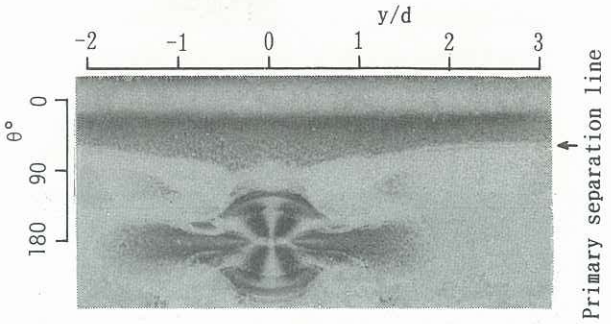

(a) Oil-film pattern

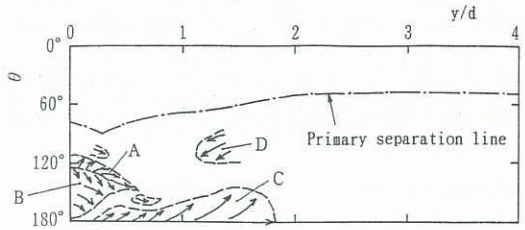

(b) Sketch of surface flow

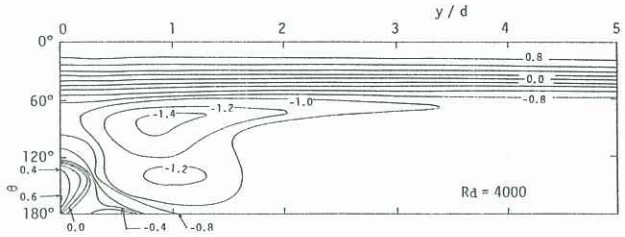

(c) Contour map of surface pressure

Fig. 3 Surface flow pattern of upstream cylinder

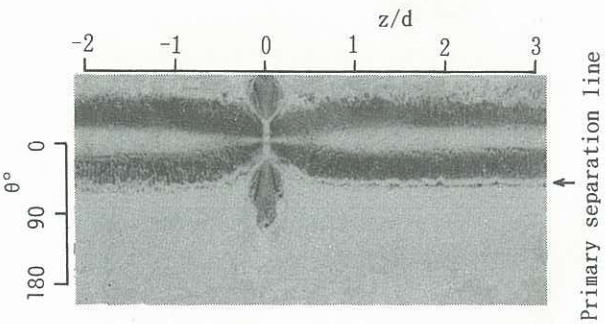

(a) Oil-film pattern

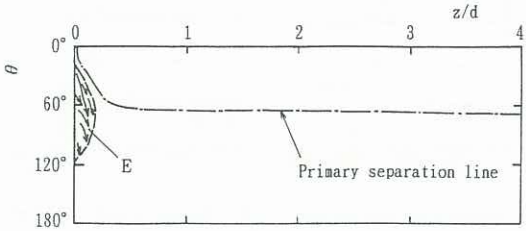

(b) Sketch of surface flow

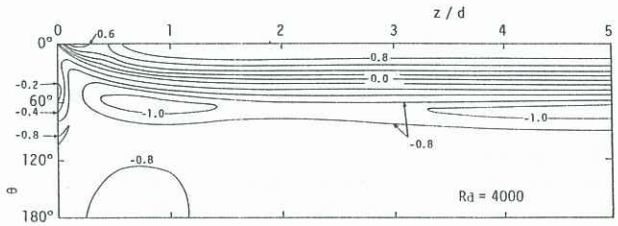

(c) Contour map of surface pressure

Fig. 4 Surface flow pattern of downstream cylinder

ders. Variation in the range of $y/d \leqq 4$ and $z/d \leqq 4$ corresponded with the oil-film pattern mentioned above. The spanwise variation in the range of $y/d \geqq 4$ and $z/d \geqq 4$ is almost negligible.

Drag coefficient

Fig. 6 shows the spanwise variation of the local pressure drag coefficient Cd in each y/d plane of the upstream cylinder and in each z/d plane of the downstream cylinder. The drag coefficient Cd in the upstream cylinder is almost zero in the y/d=0 plane where the recovery of surface pressure behind the cylinder is very large. Cd takes a maximum value in the y/d=1 plane where the surface pressure behind the cylinder becomes minimum. The maximum value of Cd is about 30% larger than that of a single cylinder. The drag coefficient Cd in the downstream cylinder in the range of $z/d \leqq 4$ is fairly small because of the bleed flow in the vicinity of the cross region, in spite of the upstream movement of the primary separation line. The drag coefficient Cd in the upstream and downstream cylinders in the range of $y/d \geqq 4$ and $z/d \geqq 4$ gradually approaches that of a single cylinder as y/d and z/d increase, but Cd in the positions y/d=15 and z/d=15 remains slightly smaller than that of a single cylinder.

Vortex shedding

Fig. 7(a), (b) show the spectral energy distribution measured in the wake along the axes of the upstream and downstream cylinders respectively.

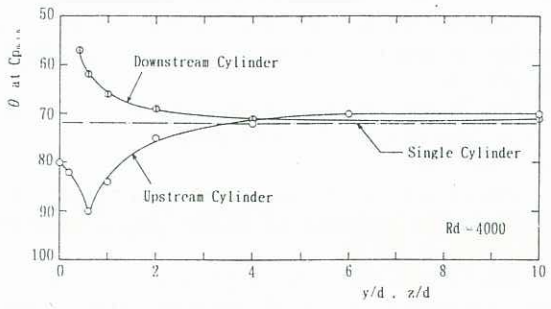

Fig. 5 Spanwise variation of minimum pressure position

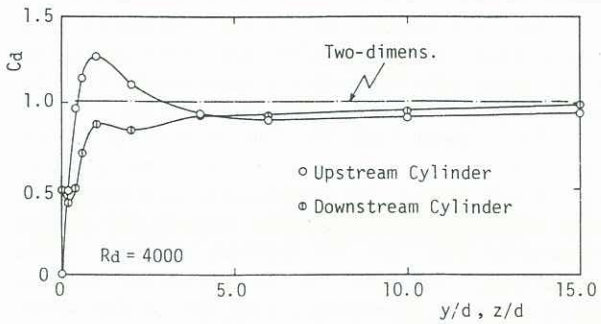

Fig. 6 Spanwise variation of local drag coefficient

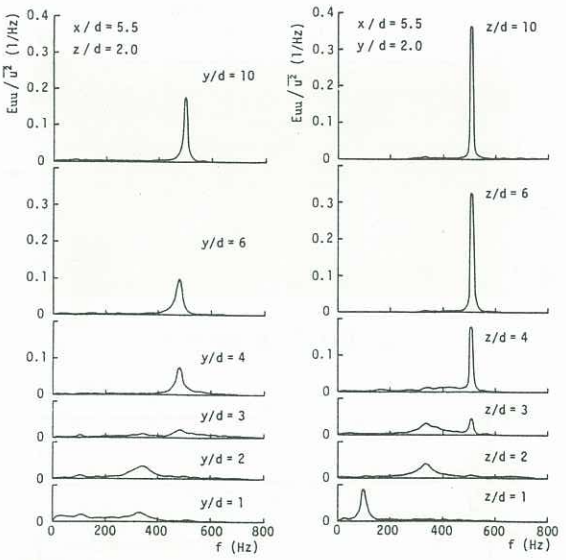

(a) Upstream cylinder (b) Downstream cylinder
Fig. 7 Spectral energy distributions in each spanwise position

Since the excellent 500 Hz frequency corresponds to the Strouhal number of the single cylinder, the spectrum peak found at about $y/d \fallingdotseq 4$ and $z/d \fallingdotseq 4$ expresses the existence of Karman vortex shedding. This has been conformed by the flow visualization carried out in the water tunnel as shown in Fig. 8(a), (b). It seems that the end of Karman vortices near the cross region are connected to one another by U-shaped vortices. On the other hand, nothing was observed in the wake of the cross region close to the contact point, where the spectrum peak at a frequency of about 330 Hz and 100 Hz is present. These two kinds of frequency seem to suggest the shedding frequency of the unsteady streamwise vortices generated by the secondary flow. But this paper does not refer to the behavior of these streamwise vortices. A locking-on between Karman vortices shed from the four cylinder parts away from the contact point was examined by four I-type hot wire sensors. Fig. 9 shows the simultaneous sampling of fluctuating velocity in the four positions A, B, C, D away from the cross region. This means that the phase of these vortices shed in the wake of the four cylinder parts away from the contact point is not correlated with one another.

Conclusions

The flow around two circular cylinders forming a cross in contact with each other in the uniform stream was investigated experimentally. The main results can be summarized as follow:

It is known that the flow pattern on the surface of the two cylinders in the range of about $y/d \leqq 4$ and $z/d \leqq 4$ is considerably different from that of a single cylinder. For example, the primary separation line on the upstream cylinder moves downstream, and one on the downstream cylinder moves upstream. A secondary flow due to the strong bleed flow near the cross region is present.

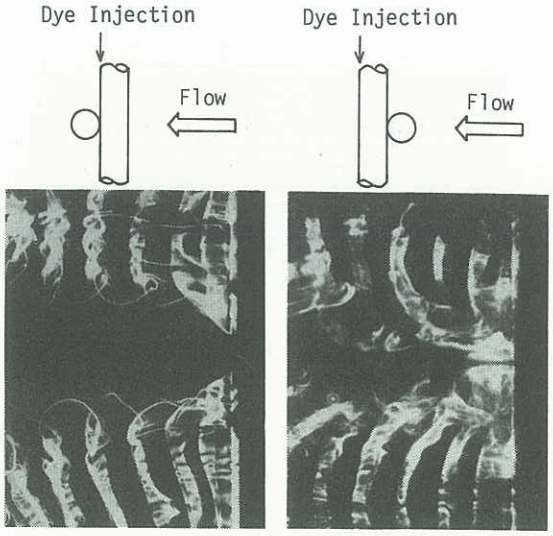

(a) Upstream cylinder (b) Downstream cylinder
Fig. 8 Visualization of Karman vortex shedding

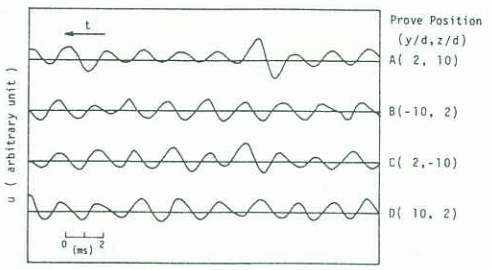

Fig. 9 Simultaneous sampling of fluctuating velocity

Therefore, the surface pressure distributions on the rear side of the upstream cylinder and on the front side of the downstream cylinder in the cross region take on characteristic variations.

The local drag coefficient of each cylinder is lower than that of a single cylinder except in the plane of about $y/d=1$ of the upstream cylinder.

The vortex shedding frequency in the four cylinder parts away from the contact point is almost equal to that in a single cylinder, but the phase of these shedding vortices is not correlated with one another.

References

ZDRAVKOVICH, MM(1983)Interference between two circular cylinders forming a cross. J Fluid Mech, 128, 231-246.

FOX, TA and TOY, N(1988)The generation of turbulence from displaced cross-members in uniform flow. Experiments in Fluids, 6, 172-178.

FOX, TA and TOY, N(1988)Fluid flow at the center of a cross composed of tubes. Int J Heat and Fluid Flow, 9, 53-61.

FOX, TA(1991)Wake characteristics of two circular cylinders arrenged perpendicular to each other. J Fluids Engineering, Trans ASME, 113, 45-50.